The Canadian Mineralogist
Vol. 33, pp. 569-583 (1995)

COMPARISON OF PETROGENETIC PROCESSES BETWEEN THE WEST VALLEY SEGMENT OF JUAN DE FUCA RIDGE AND THE ADJACENT HECK CHAIN OF SEAMOUNTS: DETAILED ELECTRON-MICROPROBE STUDY AND NOMARSKI INTERFERENCE IMAGING OF PLAGIOCLASE

NANCY A. VAN WAGONER AND MATTHEW I. LEYBOURNE*

Department of Geology, Acadia University, Wolfville, Nova Scotia B0P 1X0

THOMAS H. PEARCE AND CATHY E. TIMMS

Department of Geological Sciences, Queen's University, Kingston, Ontario K7L 3N6

ABSTRACT

We studied plagioclase phenocrysts from West Valley, the Endeavour Ridge and the Heck chain of seamounts of the northern Juan de Fuca Ridge using Nomarski imaging and detailed electron-microprobe scans in order to further document differences between magma-chamber processes in ridge and seamount environments. Chemical and textural variations in the zonation of plagioclase phenocrysts and megacrysts provide insights into the pre-eruptive history of the relevant magmas. Both seamount and ridge samples exhibit texturally complex patterns of zoning. Plagioclase phenocrysts from the seamounts, however, vary by less than 9% An content, and there is little measurable variation in An content within zones or between zones. The textures and chemistry can be accounted for by changes in temperature and pressure as the magma rose to the surface, or back mixing involving very similar magmas. In contrast, ridge samples vary by up to 21% An content. In some cases, it is possible to correlate resorption surfaces with chemical variations, providing evidence for the timing of mixing and the minimum number of magmas involved. The Endeavour Ridge rocks have not preserved mineralogical evidence for mixing, possibly owing to more efficient mixing associated with robust volcanism.

Keywords: plagioclase, Nomarski, mineralogy, Juan de Fuca Ridge, seamounts, rift, magma mixing.

SOMMAIRE

Nous avons étudié les phénocristaux de plagioclase provenant de West Valley, de la crête Endeavour, et de la chaîne de guyots de Heck sur le secteur nord de la crête Juan de Fuca. Notre étude, fondée sur images de Nomarski et des données chimiques obtenues par microsonde électronique, visait à préciser les différences dans les processus au niveau de la chambre magmatique dans les deux milieux, soit guyot et crête. Les variations texturales et compositionnelles dans la zonation des phénocristaux et des mégacristaux de plagioclase permettent de décrire certains aspects de l'évolution pré-éruptive des magmas. Les échantillons de plagioclase des deux milieux font preuve de zonation complexe. La composition de ceux du guyot ne varie que légèrement (moins que 9% en teneur du pôle anorthite), et à peine à l'intérieur d'une seule zone ou d'une zone à l'autre. Les textures et la constance en composition pourraient bien s'expliquer par des changements en température et en composition pendant la mise en place du magma, vers la surface, ou par mélange de magmas très semblables. Par contre, l'hétérogénéité des échantillons de plagioclase de la crête est plus grande, atteignant 21% en teneur du pôle anorthite. Il nous est possible d'établir un lien entre certaines surfaces de résorption et des variations importantes en composition, ce qui semble indiquer les étapes de mélanges magmatiques et le nombre minimum de liquides impliqués. Les roches de la crête Endeavour ne conservent aucun indice minéralogique de mélange, peut-être à cause de l'efficacité du phénomène associé à un volcanisme plus vigoureux.

(Traduit par la Rédaction)

Mots-clés: plagioclase, Nomarski, minéralogie, guyots, rift, mélange de magmas, crête Juan de Fuca.

* Present address: Ottawa–Carleton Geoscience Centre, Department of Geology, University of Ottawa, 161 Louis Pasteur Drive, Ottawa, Ontario K1N 6N5.

INTRODUCTION

Previous studies of mid-ocean-ridge basalt (MORB) have shown that the phenocryst phases provide insight into the pre-eruptive history of the relevant magmas (Kuo & Kirkpatrick 1982). Plagioclase phenocrysts are particularly useful because they settle out of the coexisting melt at slower rates than olivine and clinopyroxene and, owing to similar density, may even float in the magma (Elthon 1984). Plagioclase phenocrysts are capable of recording subtle variations in the conditions of crystallization and are therefore very useful in elucidating such processes as magma mixing, convection and variations in temperature and pressure (Pearce *et al.* 1987, Pearce & Clark 1989, Pearce & Kolisnik 1990, Stamatelopoulou-Seymour *et al.* 1990).

Magma mixing is widely recognized as a fundamental feature of mid-ocean-ridge magma chambers (Dungan & Rhodes 1978, Kuo & Kirkpatrick 1982, Nabelek & Langmuir 1986, Hummler & Whitechurch 1988, Davis & Clague 1990). Magma mixing is recognized in the decoupling of the major and trace elements in MORB (Rhodes *et al.* 1979, Stakes *et al.* 1984, Dixon & Clague 1986). Disequilibrium compositions of phenocrysts, phenocryst morphology, complex patterns of zoning, and the occurrence of more than one population of phenocrysts within a sample are also indicative of magma mixing (*e.g.*, Rhodes *et al.* 1979, Kuo & Kirkpatrick 1982, Nabelek & Langmuir 1986, Davis & Clague 1990, Van Wagoner & Leybourne 1991).

Volcanic rocks recovered from various small off-axis seamounts adjacent to mid-ocean ridges typically lack mantle xenoliths, are on average more primitive in composition, typically lack clinopyroxene phenocrysts, and typically host relatively unzoned phenocrysts of olivine and plagioclase. These features suggest that magma mixing and crustal assimilation are of minor significance for seamount petrogenesis (Fornari *et al.* 1988, Allan *et al.* 1988, 1989, Leybourne & Van Wagoner 1991).

The purpose of this paper is to compare the patterns of zoning and growth textures in plagioclase phenocrysts from ridge and off-ridge environments, and to ascertain how these relate to petrogenetic processes, using the northern end of Juan de Fuca Ridge as an example. The sample set includes rocks from a small off-axis chain of seamounts, the active part of a spreading system, a fracture zone and a bounding axial ridge. The study involved the use of conventional petrographic techniques, electron-microprobe data and Nomarski differential interference contrast (DIC) microscopy. These techniques provide a powerful tool for the study of the pre-eruption history of MORB.

REGIONAL GEOLOGY AND SAMPLE LOCATIONS

Juan de Fuca Ridge is situated in the northeastern Pacific Ocean and has a spreading rate of 5.8 cm/yr (full rate) (Vine & Wilson 1965). The West Valley Segment is the northernmost part of Juan de Fuca Ridge and is characterized by several deep axial valleys separated by axial ridges (Fig. 1). West Valley is the current locus of spreading, whereas Middle Valley to the east is filled with turbiditic sediments derived from the North American continental margin (Davis *et al.* 1976). West Valley is only partly sediment-covered, with fresh pillow, lobate, and sheet flows exposed on the seafloor (Leybourne & Van Wagoner 1992). West Valley is bounded to the north by the Sovanco Fracture Zone and to the south by the Endeavour Offset, where West Valley forms an overlapping spreading center with the Endeavour Ridge (Fig. 1). Perpendicular to the West Valley ridge axis at the Endeavour Offset is the Heck Seamount Chain, a small off-axis chain of seamounts (Leybourne & Van Wagoner 1991).

The samples used in this study were recovered by dredging and are from the axis of West Valley (8706; 8803), Middle Ridge, the eastern bounding ridge of Middle Valley (7016–2; 7123–1), the Sovanco Fracture Zone (7115–5), the Endeavour Ridge (8601) and the Heck Seamount Chain (8801; 8802; 7016–5) (Fig. 1). Collection methods, detailed petrographic descriptions and geochemistry of the samples are given in Van Wagoner & Leybourne (1991) and Leybourne & Van Wagoner (1991). The terminology used to describe crystal texture follows Donaldson & Brown (1977) and Bryan (1979).

ANALYTICAL TECHNIQUES

Major- and minor-element geochemistry of mineral phases and volcanic glass was determined from

TABLE 1. REPRESENTATIVE COMPOSITIONS* OF CORE AND RIM OF PLAGIOCLASE

Sample #		SiO_2	Al_2O_3	FeO	MgO	CaO	Na_2O	Total	An	Ab
8802-03	core	47.45	31.60	0.49	0.23	17.39	1.82	98.98	84.1	15.9
	rim	50.24	29.85	0.62	0.37	15.71	2.80	99.58	75.6	24.4
8802-03	core	48.74	31.06	0.51	0.24	16.92	2.20	99.67	81.0	19.0
	rim	52.07	27.87	0.95	0.50	14.20	3.50	99.09	69.2	30.8
7016-5-A	core	46.78	31.63	0.51	0.20	18.16	1.48	98.76	87.1	12.9
	rim	52.18	27.96	1.03	0.53	14.19	3.46	99.35	69.4	30.6
8802-10	core	47.95	31.83	0.46	0.33	17.48	1.89	99.94	83.6	16.4
	rim	48.51	32.08	0.56	0.13	16.61	1.82	99.70	83.5	16.5
8802-10	core	47.60	31.65	0.44	0.24	17.60	1.88	99.40	83.8	16.2
	rim	50.19	29.40	0.74	0.35	15.36	2.87	98.90	74.7	25.3
8706-05	core	48.48	31.78	0.66	0.14	15.85	2.55	99.45	77.5	22.5
	rim	50.16	29.90	0.68	0.24	14.41	3.20	98.58	71.3	28.7
8706-05	core	49.45	30.53	0.49	0.27	15.18	2.89	98.81	74.4	25.6
	rim	50.68	29.49	0.73	0.36	13.93	3.37	98.56	69.6	30.4
8803-01	core	47.91	31.82	0.38	0.22	17.50	1.79	99.62	84.4	15.6
	rim	56.44	24.65	1.79	1.15	11.41	4.91	100.36	56.2	43.8
7115-5-C	core	46.33	33.29	0.46	0.18	18.69	1.17	100.12	89.8	10.2
	rim	51.53	29.14	0.47	0.16	14.63	3.30	99.23	71.0	29.0
7115-5-C	core	46.64	32.89	0.30	0.20	18.37	1.41	99.80	87.8	12.2
	rim	52.18	29.00	0.72	0.39	14.60	3.45	100.34	70.1	29.9
7016-2-19	core	47.23	31.96	0.30	0.23	17.83	1.55	99.11	86.4	13.6
	rim	53.46	28.41	0.78	0.58	14.23	3.64	101.09	68.4	31.6

* Compositions are derived from electron-microprobe data, and are quoted in wt%.

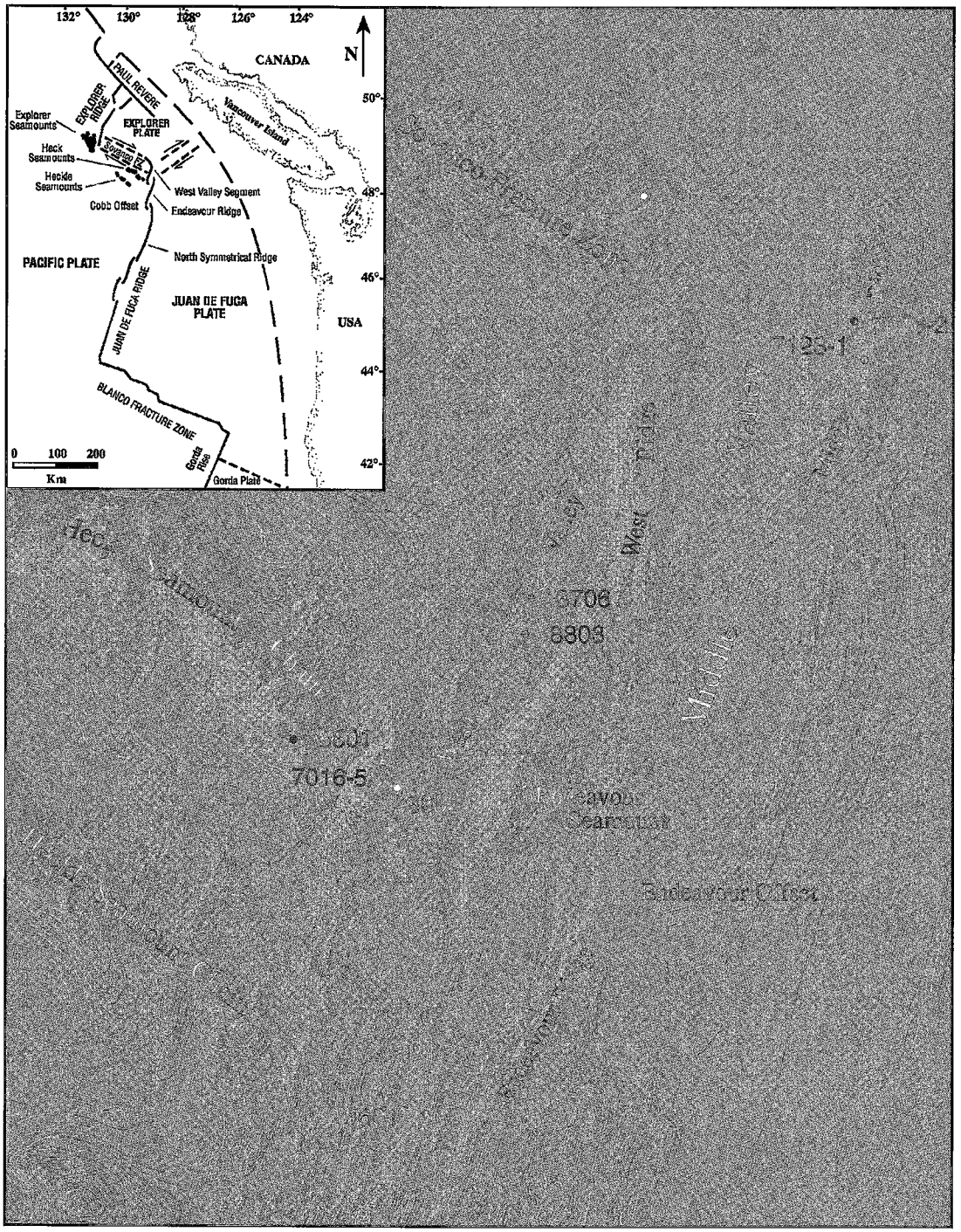

FIG. 1. Seabeam bathymetry map of the study area (from Davis *et al.* 1987) showing the sample locations and main tectonic components. The regional setting of the study area is shown on the inset map.

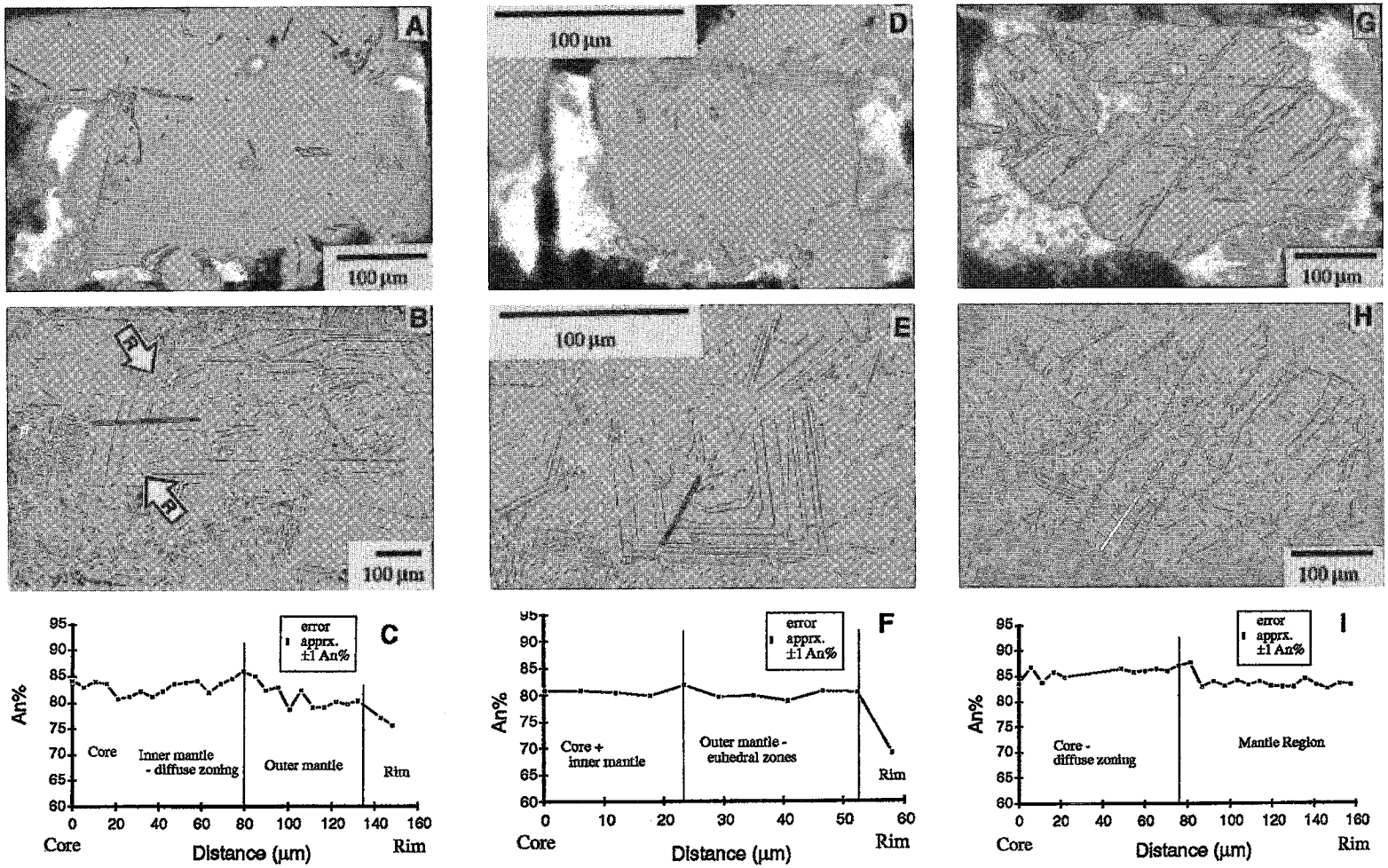

FIG. 2. (A) Cross-polarized light (XPL) image of a plagioclase phenocryst from East Peak sample 8802–03. (B) Nomarski DIC image of the above phenocryst. Note the complex zoning and numerous inclusions of glass in the core of the crystal. Resorption surfaces [denoted R on figure] are delineated by angular unconformities. (C) Core-to-rim variation in An content in the above crystal. (D) XPL image of a plagioclase phenocryst from East Peak, sample 8802–03. (E) Nomarski DIC image of the above phenocryst. (F) Core-to-rim variation in An content in the above crystal. (G) XPL image of a plagioclase phenocryst from East Peak, sample 8802–10. (H) Nomarski DIC image of the above phenocryst. (I) Core-to-rim variation in An content in the above crystal.

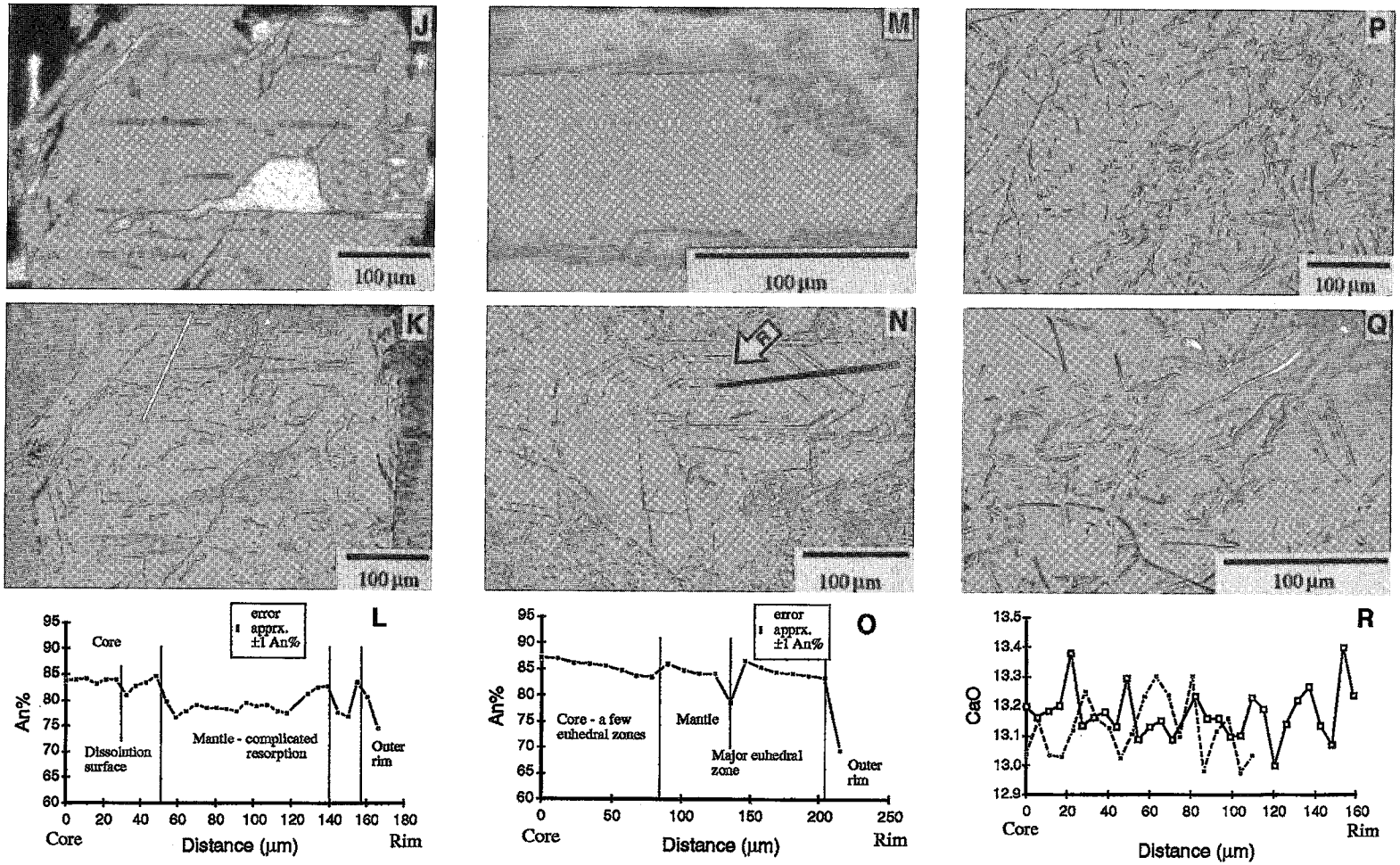

FIG. 2 (continued). (J) Crossed-polars image of a plagioclase phenocryst from sample 8802–10, East Peak. A "wormy" pattern of zoning is apparent in this conventional view. (K) Nomarski DIC image of the above crystal. The complexity in zoning pattern is greatly enhanced in this image. (L) Core-to-rim variation in An content in the above crystal. (M) XPL image of a plagioclase phenocryst from East Peak, sample 8802–10. (N) Nomarski DIC image of the above phenocryst. The sharp euhedral zones are cut only once by a resorption surface [denoted R on figure]. (O) Core-to-rim variation in An content in the above crystal. (P) Nomarski DIC image of acicular plagioclase microlites in "swirly" glass from sample 8801–01, Heck chain of seamounts. (Q) Same as above but enlarged. (R) Line scans of Ca concentrations in glass in sample 8801–01. Note that the variation is less than the accuracy of the electron microprobe.

standard carbon-coated polished thin sections using a JEOL 733 four-spectrometer electron microprobe at Dalhousie University. All analyses were carried out with a 15 kV electron acceleration potential and a 12.4 nA sample current using a focused beam of electrons (1 mm). Mineral standards [sanidine (Al, Si), jadeite (Na), kaersutite (Mg, Ti), garnet (Fe)] were used for the quantitative analysis of plagioclase. An in-house sideromelane standard was used for the analysis of glass. The data were reduced using an on-line Link matrix-correction program (ZAF). Linear traverses from core to rim of plagioclase phenocrysts and megacrysts were carried out using an automated energy-dispersion system. Representative electron-microprobe data are given in Table 1. Full data-sets are available from the Depository of Unpublished Data, CISTI, National Research Council of Canada, Ottawa, Ontario K1A 0S2.

The Nomarski differential interference contrast (DIC) imaging technique was used to highlight the subtle variations in plagioclase zoning. This technique provides information on zoning characteristics that are important in the interpretation of residence time in magma chambers, and of episodes of growth or dissolution during reaction with the magma. Features of rapid growth can be distinguished from features indicative of slower growth.

The Nomarski imaging technique involves etching of polished thin sections with concentrated fluoboric acid (HBF_4), followed by neutralization with Na_2CO_3. This process preferentially leaches the Ca-rich portions of plagioclase crystals, producing a microtopographic relief that allows observation of small variations in the An content. Owing to this preferential etching, the Nomarski technique gives qualitative compositional information.

Results on Seamount Rocks

In general, the rocks are aphyric to very sparsely phyric, with only a few samples containing more than 2% phenocrysts. Megacrysts are rare, and commonly host a fluid-inclusion-charged core (*e.g.*, Fig. 2G). Phenocrysts are slightly more common than megacrysts. They are smaller, bladed to equant, and commonly in glomerophyric relationships. Microphenocrysts are common in pillow basalts (Figs. 2P, Q), but rare to absent in glassy fragments of sheet flows.

Nomarski DIC images of plagioclase phenocrysts from rocks from East Peak show several interesting features. Where there is an obvious core, it is characterized by a fritted texture and diffuse zonation (Figs. 2B, E, H). It shows little chemical variation (*e.g.*, Figs. 2C, F, I). The plagioclase crystals are typically characterized by resorption surfaces at the core–mantle boundary, resulting in angular unconformities (Figs. 2B, E, H, K, N). However, there typically is little chemical change across these boundaries (3.2 – 8.6% An).

The mantle regions of the majority of the plagioclase crystals studied are characterized by regular, conformable zones that show up clearly in the Nomarski images (Figs. 2B, E, H, N). Rarely, phenocrysts display "packages" of euhedral zones bounded by a distinct anhedral surface that forms angular unconformities with subsequent growth-zones (Figs. 2B, K). In either case, there is little chemical variation across zones or dissolution surfaces, within the accuracy of the microprobe determinations (Figs. 2C, F, I, O). There typically is a sharp drop in An content at the rim of the crystals.

Some of the samples from the seamounts show an unusual texture in the glassy flow-margins (Figs. 2P, Q), which usually etches without relief. The texture gives the glass a "swirly" appearance, with gradational contacts between variably etched bands. Two detailed traverses across the glass in sample 8801–01 were carried out with the electron microprobe at 5-mm intervals. Whereas the etching by HBF_4 provides a textural indication of chemical heterogeneity, the microprobe results show only subtle chemical variations, which are near its detection limit (Fig. 2R; total variation in CaO in the two traverses is 0.33 and 0.40 wt%).

Results on Ridge Rocks

West Valley North (8706–05, 8706–07)

Although the margin of many phenocrysts exhibits reaction with the melt, euhedral phenocrysts are common. The plagioclase phenocrysts can be divided into three groups based on their size and textures. Type-1 phenocrysts range from 1 to 2 mm in length, and are rare. Their texture is characterized by a complex inclusion-charged core enclosed by diffuse zones (Figs. 3A, B). Diffuse zones are present in the interior of the type-1 phenocryst analyzed (Fig. 3B). This portion of the crystal is separated from the younger portion by a resorption event marked by a rounded interface associated with angular unconformities between the core and the mantle (large arrow, Fig. 3B). The edge of the core is marked by a decline in An content of 8% (Fig. 3C). Anorthite content increases sharply at the edge of the surrounding zone of dissolution and declines radically through that zone (12.7% An). Note that although the sharp zones outside this dissolution area are not euhedral, most are conformable, indicating that 1) growth was nearly continuous, and 2) only a small change in chemistry occurs across these sharp boundaries (3.5% An). In general, this type of crystal shows the strongest variation in An content in the core and mantle of the West Valley North rocks (20.5% An) (Fig. 3C).

Type-2 phenocrysts are about 0.4 to 1 mm in length and represent about 10 to 15% of the total population of phenocrysts. They are characterized by a core that is more calcic than the mantle that surrounds them. A distinct rounded resorption-induced surface characterized by numerous angular unconformities separates this core from the mantle. The resorption was apparently so intense that the older part of the crystal inside this surface was reduced to a crystal fragment with an irregular dissolution-surface that later served as a nucleus for the present crystal (Fig. 3E). The core is calcic and fairly uniform in composition ($An_{79.3-81.9}$). There is a large decrease in An content across this resorption surface, down to $An_{66.9}$. Dissolution zones occur within the mantle, separating "packages" of fine euhedral zones. There is a general increase in An content throughout the mantle region, then a sharp decrease at the rim (Fig. 3F).

Type-3 phenocrysts represent the microphenocryst population and are the most abundant, comprising up to 80 to 85% of the plagioclase crystals present. Crystals in this group exhibit 30- to 160-mm-thick "packages" of mostly conformable euhedral zones; these zones are periodically interrupted by distinct, single anhedral zones associated with angular unconformities. This regular arrangement of "packages" of euhedral zones bounded by dissolution-induced zones appears to be cyclic throughout most of these crystals (Figs. 3E, K). Each bounded "package" consists of 10 to 12 euhedral zones. The core-to-mantle variation in An in these crystals is minor ($An_{68.4-74.5}$), with the dissolution surfaces marked by only subtle changes in chemistry (Figs. 3I, L, O). In rare cases, the anhedral zones are absent, and the crystals are entirely made up of conformable euhedral zones. The entire radius of such crystals probably represents one "package" of euhedral zones in the above crystals (Fig. 3N), a feature noted previously in plagioclase phenocrysts from Mt. St. Helens (Pearce *et al.* 1987).

West Valley Central (8803–01)

Plagioclase is the most common mineral in these very glassy rocks and typically occurs as equant megacrysts. Smaller bladed phenocrysts are less common, and microphenocrysts are rare. The core of the analyzed megacryst shows a hieroglyphic texture, indicative of resorption, and diffuse compositional zones (Figs. 3P, Q). The edge of the core grades into distinct zones that show an increase followed by a decline in An content, from 88.1 to 68.4% (Fig. 3R). The irregular rim is a complex intergrowth of two plagioclase compositions, as indicated by differences in relief and small variations in measured An content (68.4 – 71.5%). The outermost skeletal zone surrounds and fills the embayments of the adjacent zone and has a relatively low An content (56.2%) (Figs. 3P–R).

Middle Ridge (7016–2–19)

Plagioclase megacrysts are the dominant crystal form, are typically inclusion-rich, show minor reaction with the melt at their margins and commonly form complex glomerophyric masses. Microphenocrysts are volumetrically subordinate, and phenocrysts are rare.

The megacrysts have large core areas that commonly show numerous inclusions (Fig. 4B), diffuse zoning (Fig. 4E), and hieroglyphic textures (Fig. 4H). The cores are all very calcic ($An_{86.3-92.2}$). The boundaries between the core and mantle are typically marked by a resorption-induced surface with moderate to little chemical variation across the boundary (1.9 – 4.5% An; Figs. 4C, F, I). The mantle regions also are complex, with well-defined hieroglyphic zones (Fig. 4B); angular unconformities with subsequent growth fill in the embayments (Figs. 4E, H). The crystals show moderate variation in An content across the core and mantle regions (6.5% An, Figs. 4A–C; 11.5% An, Figs. 4D–F; 10.1% An, Figs. 4G–I).

Sovanco Fracture Zone (7115–5–C)

Large, tabular euhedral to subhedral plagioclase megacrysts are dominant. Their margins are typically embayed and anhedral, cores are inclusion-rich, and are commonly in complex glomerocrysts. Microphenocrysts are common, and phenocrysts, rare.

The complexly zoned megacrysts show prominent resorption-induced zones; many of the larger crystals have a distinct two-stage history (Figs. 4J–L, M–O). They have a large core with diffuse and, commonly, inclusion-charged zones. In this way, they are similar to the megacrysts from Middle Ridge sample 7016–2–19. The cores are calcic ($An_{86.4-89.4}$). The boundary between the core and mantle is marked by a subtle reaction-surface and a moderate drop in An content (6 – 10% An). The outer mantle areas are characterized by a resorption surface and fine zones that are conformable to the reaction surface. The fine zones are characterized by a sharp drop in An content (11–16% An). This drop is followed by another sharp drop at the rim, to $An_{61.1-61.5}$. Both crystals appear to have undergone similar histories, given the broadly similar compositional profiles and ranges in core-to-rim variation (core and mantle compositions vary over the range $An_{77.1-89.4}$ and $An_{75.6-89.7}$; rim compositions vary over the range $An_{73.0-61.1}$ and $An_{71.0-61.5}$; Figs. 4L, O).

Endeavour Ridge (8601–02)

Plagioclase occurs as rare small phenocrysts (≤ 300 mm). Plagioclase microlites are common. The phenocrysts are generally euhedral to subhedral, tabular to bladed, rarely with a corroded core. Figures 5A–B shows a typical phenocryst of plagio-

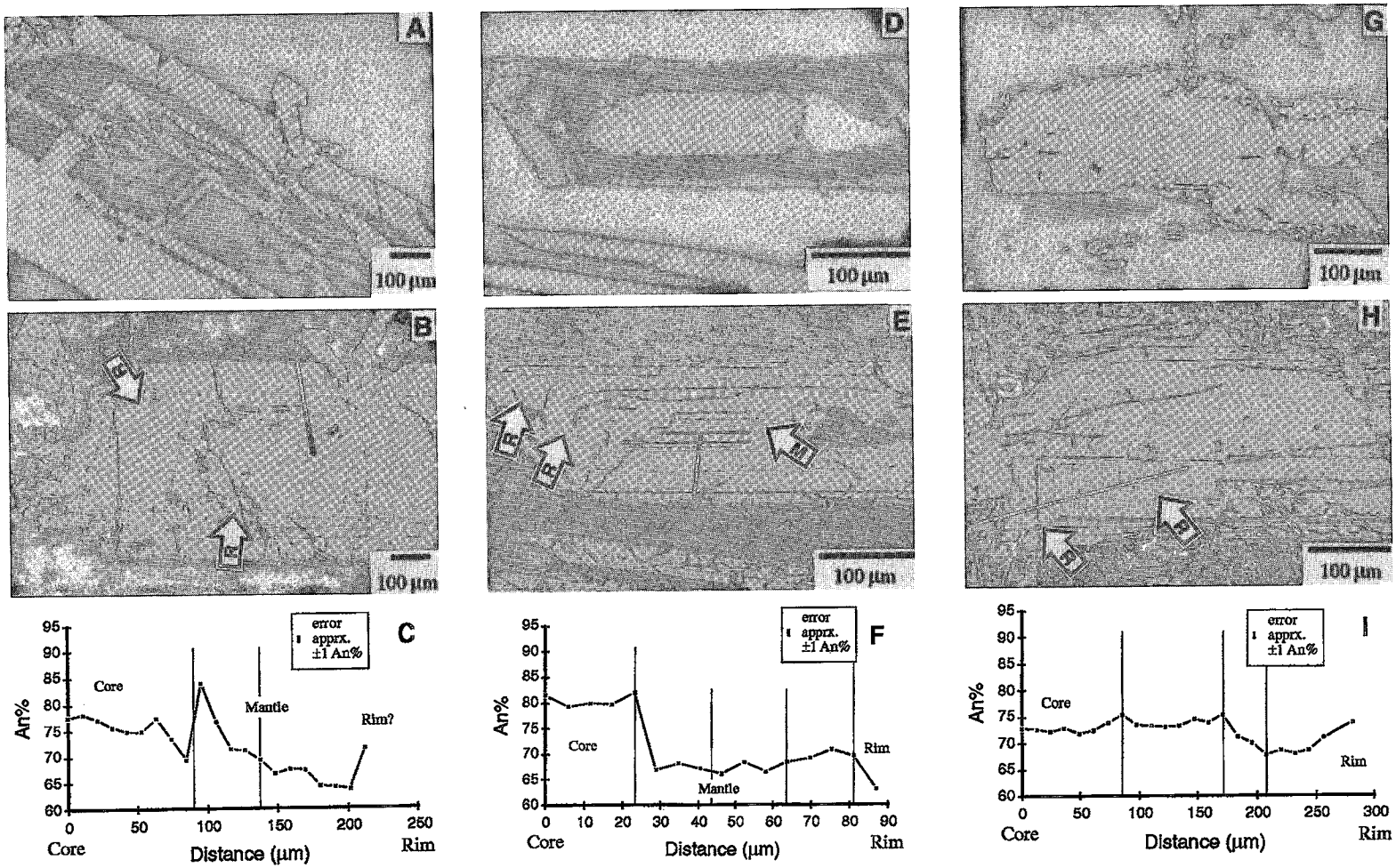

FIG. 3. (A) XPL view of a plagioclase crystal from sample 8706–05, West Valley North. This crystal is marked by a distinct calcic core. Note also the zoning near the rim of the crystal. (B) Nomarski DIC image of above crystal, showing prominent resorption-induced surfaces [denoted R on figure]. (C) Core-to-rim variation in An content in the above crystal. (D) XPL view of a plagioclase crystal from sample 8706–05, West Valley North. (E) Nomarski DIC image of the above phenocryst. Note the resorption surface at the core boundary [denoted M], and less distinct resorption-induced surfaces in the mantle [denoted R]. (F) Core-to-rim variation in An content in the above crystal. (G) XPL view of a plagioclase crystal from sample 8706–05, West Valley North. (H) Nomarski DIC image of the above phenocryst. This crystal has been sectioned very close to its core, and euhedral zones can be seen to dominate from the core to the rim, with subtle dissolution-induced zones [denoted R]. (I) Core-to-rim variation in An content in the above crystal.

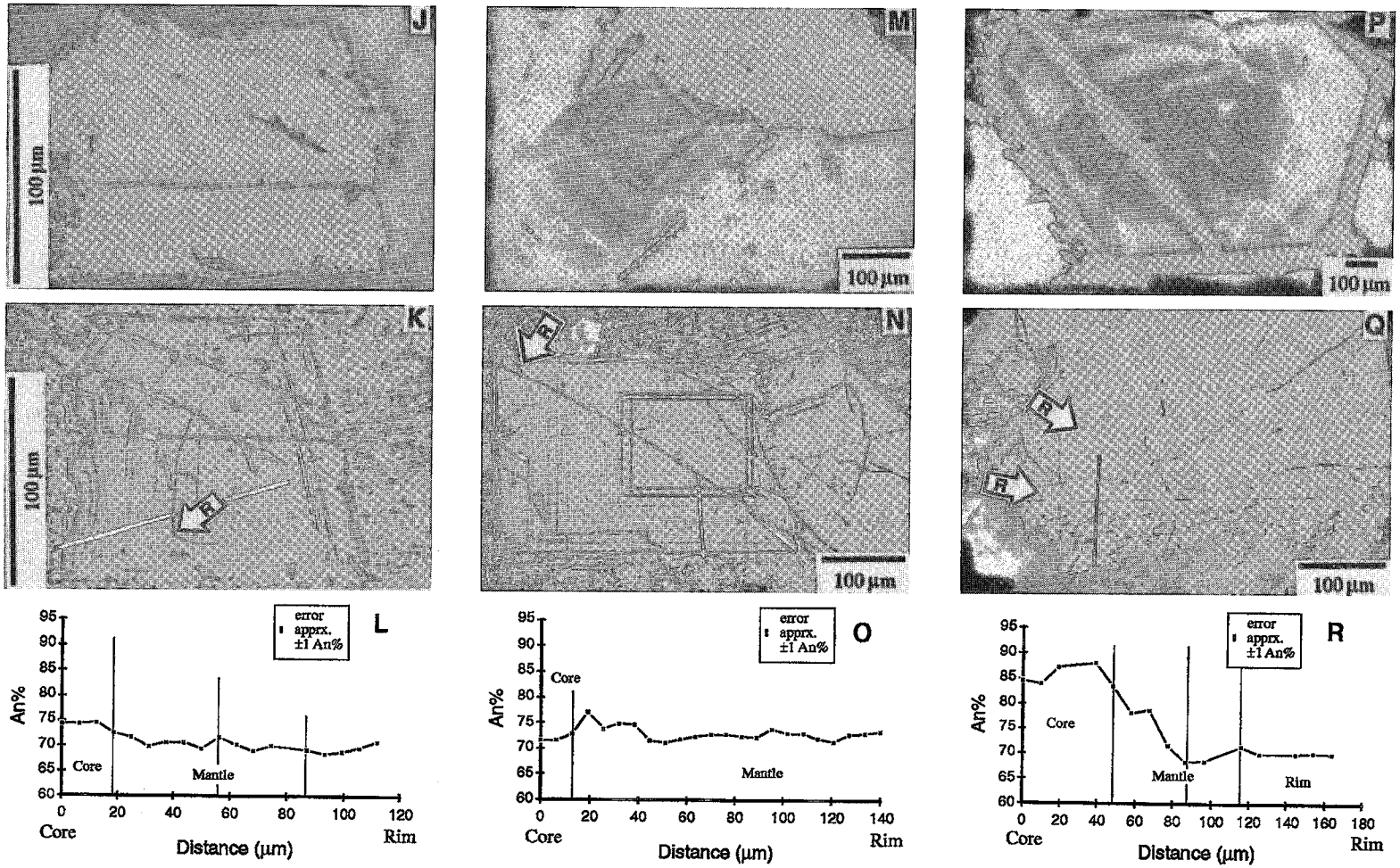

FIG. 3 (continued). (J) XPL view of a plagioclase crystal from sample 8706–05, West Valley North. (K) Nomarski DIC image of the above phenocryst. A number of "packages" of euhedral zones are bounded by zones of dissolution [denoted R on figure]. Note that the width of one of these packages is approximately the same as the width of the crystal in Fig. 4A. (L) Core-to-rim variation in An content in the above crystal. (M) XPL view of a plagioclase crystal from sample 8706–07, West Valley North. (N) Nomarski DIC image of the above phenocryst. This crystal is predominantly composed of numerous sharp, euhedral zones. One zone of dissolution is present near the rim of the crystal [denoted R on figure]. (O) Core-to-rim variation in An content in the above crystal. (P) XPL view of a plagioclase phenocryst from sample 8803–01, West Valley Central. (Q) Nomarski DIC image of the above crystal. Note resorption surfaces [denoted R on figure]. (R) Core-to-rim variation in An content in the above crystal.

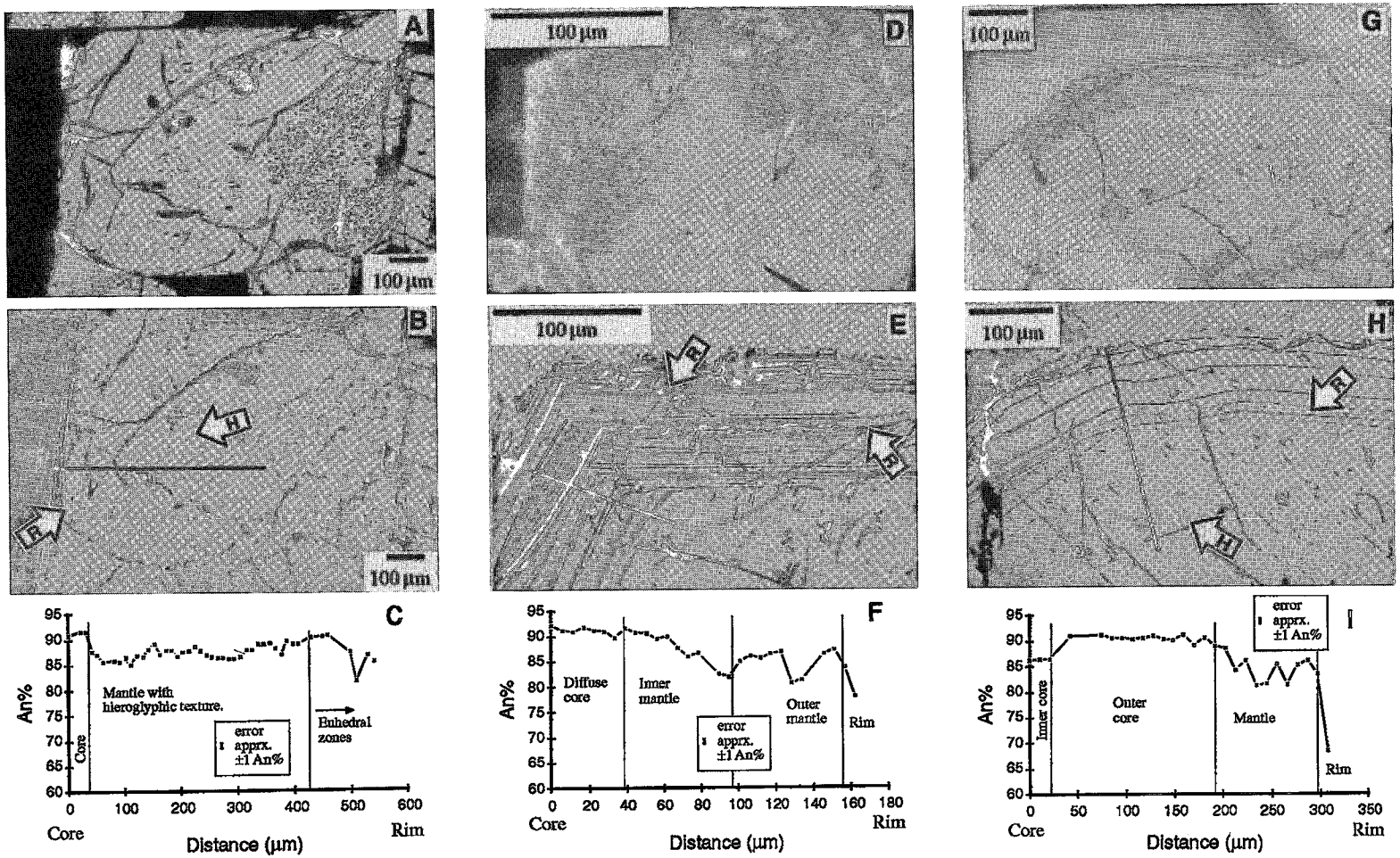

FIG. 4. (A) XPL view of a plagioclase phenocryst from sample 7016–2–19, Middle Ridge. A glass inclusion-charged core and two zones with glass inclusions are visible. Compositional zoning is not evident. (B) Nomarski DIC view of the above crystal. Note the hieroglyphic textures [denoted H on figure] and dissolution surfaces [denoted R on figure]. (C) Core-to-rim variation in An content in the above crystal. (D) XPL view of a plagioclase crystal from sample 7016–2–19, Middle Ridge. (E) Nomarski DIC image of the above phenocryst, with resorption surfaces [denoted R on figure]. (F) Core-to-rim variation in An content in the above crystal. (G) XPL view of a plagioclase crystal from sample 7016–2–19, Sovanco Fracture Zone. (H) Nomarski DIC image of the above phenocryst. Diffuse "hieroglyphic" texture is present at the edge of the core [denoted H on figure]. A resorption event also occurred to produce the angular unconformity [denoted R on figure]. (I) Core-to-rim variation in An content in the above crystal.

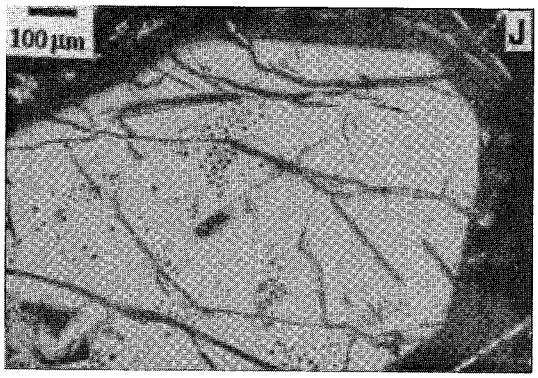

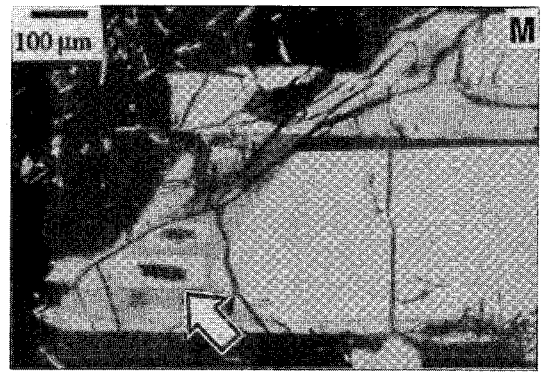

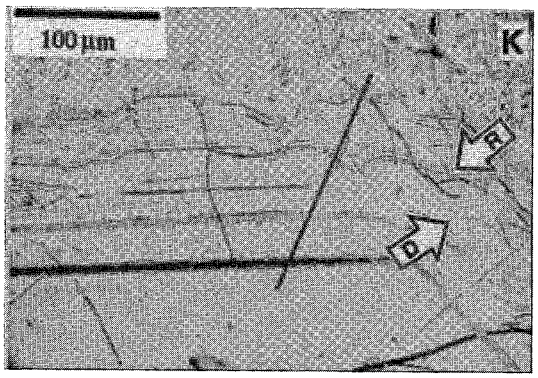

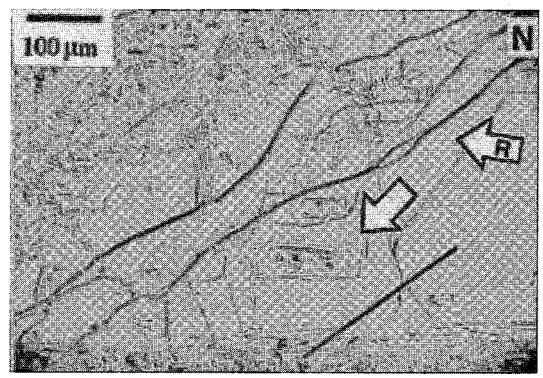

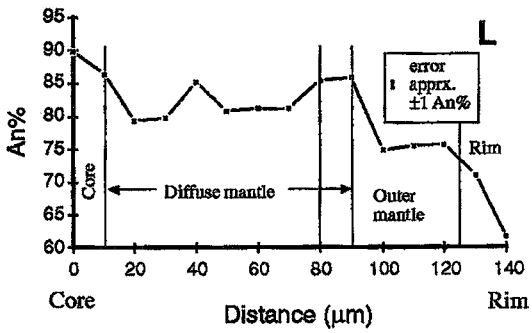

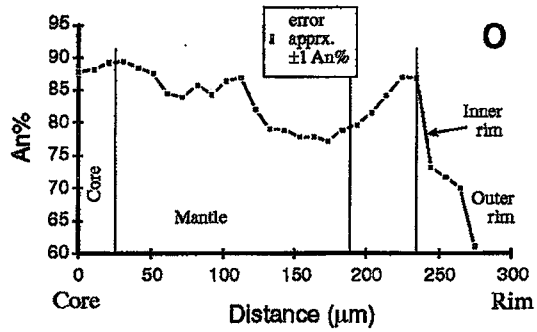

FIG. 4 (continued). (J) XPL image of a plagioclase phenocryst from sample 7115–5–C, Sovanco Fracture Zone. (K) Nomarski DIC image of the above crystal. Detail of the zoning is enhanced in this image. Note the strong and diffuse resorption-induced surfaces [denoted R and D, respectively]. (L) Core-to-rim variation in An content in the above crystal. (M) XPL image of a plagioclase phenocryst from sample 7115–5–C, Sovanco Fracture Zone. Compositional zoning is evident at the edge of the crystal. Note the zoning around the large glass inclusions (arrow). (N) Nomarski DIC image of the above crystal. Note also the fine-scale sharp zoning that surrounds the large devitrified glass inclusions (arrow) and resorption surfaces [denoted R on figure]. (O) Core-to-rim variation in An content in the above crystal.

clase with its fine-scale euhedral zoning and sector zoning. This crystal has apparently had a very simple history and contains only a small, diffuse core. The core area is slightly more sodic ($An_{74.9–75.6}$) than the euhedral zones ($An_{78.8–80.3}$), with the exception of the outer rim ($An_{71.9}$). The euhedral zones display little variation in chemistry (1.5% An).

Middle Ridge (7123–1)

Plagioclase crystals are dominantly euhedral, bladed to acicular and skeletal microphenocrysts. The microphenocrysts typically have a small core-area bounded by a rounded resorption-induced surface. Little or no zoning is evident in the Nomarski images, and chemical changes are minor (core-to-rim variation $An_{71.2} \rightarrow An_{64.6}$).

Discussion

Seamount rocks

The seamount rocks contain rare plagioclase megacrysts and phenocrysts. Although many plagioclase phenocrysts in samples from seamounts have simple patterns of zoning and show little evidence of a complex history (*e.g.*, Fig. 2E), megacrysts commonly show resorption-induced features and, in some cases, exhibit good textural evidence for complex histories (*e.g.*, Figs. 2J, K). However, the detailed electron-microprobe scans show that the extent of chemical variation within a megacryst is typically small. The resorption-induced surfaces and reaction textures (Fig. 2) suggest convectional overturn, and back-mixing between two magmas that are very closely related (*i.e.*, cogenetic). This proposal is consistent with the slight chemical variation that accompanies the resorption events and with the primitive (Mg# in the range 63–69; Leybourne & Van Wagoner 1991) and aphanitic nature (Table 1) of the seamount rocks, indicating limited residence-times in subcrustal magma-chambers (Leybourne & Van Wagoner 1991). Back-mixing implies that the magma conduit(s) must have been sufficiently large and persistent to sustain overturns or mixing of different magma-batches. The degree of dissolution that occurs at the edge of euhedral zoning-sequences seems to be less than the amount considered to be caused by mixing of chemically different magmas (Pearce & Kolisnik 1990). Rare phenocrysts have a clearly complex history, albeit with little evidence preserved of major chemical changes possibly due to magma mixing (Fig. 2K). The large, diffuse core-areas indicate residence in magma chambers for a sufficiently long time and at sufficiently high temperatures to result in the destruction of the original patterns of zoning by diffusion (Pearce & Kolisnik 1990).

The "stair-step" effect of the zones in this crystal marks normal–oscillatory zoning. There is typically a sharp drop in anorthite content at the rim of the crystals, which is attributed to supercooling during extrusion (Kuo & Kirkpatrick 1982).

In previous studies on these seamount rocks, little within-sample variation in the Fo content of olivine phenocrysts was found for the suite as a whole (in 12 samples, Fo varied by less than 1% Fo within a phenocryst and by less than 3% Fo within a sample). In addition, the olivine phenocrysts and microphenocrysts in seamount rocks are equilibrium phases and commonly exhibit reverse zoning, due either to an increase in pressure during crystallization, which produces a higher K_D (Bender *et al.* 1978, Ulmer 1989), or to magma mixing.

If the seamount rocks represent hybrid melts, the magmas involved in the mixing process were all essentially mafic tholeiitic melts with very little variation in trace-element ratios or degree of chemical evolution, given their chemical homogeneity compared to the ridge rocks (Leybourne & Van Wagoner 1991). Alternatively, the textural and chemical variation in the plagioclase phenocrysts can be accounted for by changes in temperature and pressure during crystallization.

We considered three possible explanations for the swirly texture observed in the glassy margin of some of the seamount rocks: mixing, diffusion and instrument drift during analyses. The texture may be evidence of two physically distinct but chemically similar liquids frozen in the process of mixing. However, it is unclear whether the chemical variation observed is a function of real differences in Ca content or whether the patterns represent instrument drift of the microprobe. Curiously, this feature was not observed in some of the ridge rocks such as 8706–05, in which there is convincing mineralogical and chemical evidence for mixing (see below; Van Wagoner & Leybourne 1991). The lack of textural evidence for mixing in the glass from the ridge rocks may be due to more effective mixing within subcrustal magma-chambers compared to the seamount rocks, combined with rapid ascent from the mantle in the case of the seamount rocks compared to the ridge environment (Leybourne & Van Wagoner 1991). Alternatively, the small chemical variations in the glass may be related to crystallization of plagioclase microlites. The swirly texture would then represent chemical variation in Ca and Na as a result of diffusion between crystal and adjacent host glass.

Ridge rocks

The ridge rocks contain a variety of megacryst and phenocryst types that reflect a variety of processes. Samples from West Valley North, West Valley Central, Sovanco Fracture Zone and Middle Ridge host large megacrysts of plagioclase with large variations in

An content across resorption-induced surfaces. The megacrysts are texturally complex and commonly have moderate to large variations in An content. These features can be accounted for by mixing within magma chambers. The large diffuse cores and the presence of resorption textures in some cases indicate that the megacrysts in these rocks had long and complex histories, with sufficient residence-times to remove internal zoning. The resorption surfaces and hieroglyphic textures in the mantle regions, combined with moderate chemical changes, suggest more than one mixing event. The oscillatory zoning in the outer mantle regions of some of the crystals may be a result of convection within the magma chamber.

The zoning in the cores was probably originally much sharper, but because of long periods at high temperatures, the sharp boundaries between zones have been eliminated. Whereas it is difficult to quantify this time period, our best estimate based on analogy with magmatic systems is of the order of 10^3–10^4 years. The large size of the crystals (typically 1–3 mm) also is compatible with long periods of growth for the megacrysts. The movement of the magma from depth to a subvolcanic location was accompanied by strong resorption, possibly due to pressure release or magma mixing. Once in the subvolcanic environment, the crystals grew rapidly (with irregular but conformable fine-scale zones) and then were erupted. We find it noteworthy that the distinct zoning in the rim lies upon a prominent resorption-induced surface and can be correlated among many crystals. In some cases (West Valley North, Sovanco Fracture Zone), the combination of Nomarski DIC imagery and microprobe data allows interpretation of the minimum number of liquids involved in mixing and the relative timing of the mixing events.

The textural and mineral chemical evidence is supported by the diversity in chemistry (Mg# in the range 52–65) and porphyritic nature of many of the rocks. Other mineralogical evidence comes from chemical data on the olivine and clinopyroxene phenocrysts. Van Wagoner & Leybourne (1991) found considerable variation among these ridge rocks (in 18 samples, Fo varied by up to 4.5% Fo within a phenocryst and by up to 7.1% Fo within a sample). In addition, olivine compositions are commonly too Fo-rich to be in equilibrium with the host glass, and clinopyroxene phenocrysts also show variable and disequilibrium compositions (Van Wagoner & Leybourne 1991).

The Endeavour Ridge and Middle Ridge (7123–1) rocks are moderately evolved chemically (Mg# in the range 57.8 – 65; Van Wagoner & Leybourne 1991), yet contain simple phenocrysts and microphenocrysts of plagioclase. Their evolved compositions indicate differentiation in magma chambers. Magma mixing for these systems may be so effective and robust as to destroy any mineralogical evidence, as is the case at other medium- and fast-spreading segments along the ridge (Kuo & Kirkpatrick 1982).

Diffuse zones are present in the interior of the type-1 phenocryst analyzed (Fig. 3B), indicating that this portion of the crystal has undergone coupled diffusion and is substantially older than the mantle and rim of the crystal. In summary, type-1 phenocrysts are characterized by a long-lived core in which diffusion has destroyed any original zoning. Large chemical changes associated with resorption surfaces can be attributed to magma mixing. Type-2 phenocrysts have a distinct and strongly resorbed core lacking signs of rehomogenization. Chemical changes across resorption-induced boundaries can be attributed to magma mixing. Interestingly, across the major such boundary in the type-1 and type-2 crystals, there is a similar An content, with minor chemical variation in the outer mantle regions that can be accommodated by convective overturn. The type-3 phenocrysts are all very similar texturally and chemically (Figs. 3G–O). Small chemical variations and "packages" of euhedral zones separated by resorption surfaces can be accounted for by growth in an open and convecting magma-chamber, and are probably the normal consequence of crystal growth (Shore & Fowler, in prep.). Typically, the outer mantle regions indicate crystal growth uninterrupted by large-scale resorption or reaction, as shown by conformable zones with oscillatory zoning (Figs. 4F, I).

Type-1 and type-2 phenocrysts are interpreted as complex crystals having a xenocrystic core ($An_{78–80}$) surrounded by mantles and a rim that are cogenetic with the whole zoning patterns of the type-3 crystals, as indicated by their similar chemistry. In some cases (Figs. 3D, E, F), a strongly resorbed calcic fragment has served as a nucleus for growth of the mantle (An_{66}), which is inferred to have taken place in the hybrid liquid after mixing. Two magmas are implied for this simple-mixing model: one with An_{80} crystals (now only present as a core in type-1 and type-2 crystals), and a second, more evolved magma. We did not observe phenocrysts attributable to this second evolved magma, suggesting that more sodic phenocrysts did not survive the mixing event (Tsuchiyama 1985). This crystal shows evidence of a complex history in the core. From the edge of the core to the rim, there is a sharp decline in An content that may be indicative of a steadily fractionating magma. The drop in An content ($An_{84\rightarrow67}$) at the rim of one of the crystals is probably due to supercooling upon eruption. These microphenocrysts also typically have a skeletal form, indicative of rapid growth upon extrusion. The core may have formed during transport from a magma chamber to the surface, with minor convection in a dyke system to produce the minor resorption-induced surfaces.

Olivine crystals from these rocks show a variation in chemistry (core 81.7 – 83.8% Fo, rim 80.1 – 81.2% Fo, microphenocrysts 77.8 – 83.4% Fo; data from Van Wagoner & Leybourne 1991). Because olivine re-

equilibrates with the surrounding liquid more rapidly than plagioclase (Fisk *et al.* 1982), mixing is considered to have been followed closely by eruption. Olivine phenocrysts in these rocks also show a change in core to rim compositions (cores 80.0 – 86.7% Fo, rims 79.6 – 84.6% Fo; data from Van Wagoner & Leybourne 1991), but most compositions of rim and microphenocryst are similar.

The Endeavour Ridge is characterized by an axial high and voluminous volcanism (Van Wagoner & Leybourne 1991). The aphyric character but moderately fractionated compositions of these rocks suggest that the lavas may have evolved within open-system magma chambers. However, petrographic evidence for magma-chamber processes was not recorded in patterns of zoning because the rocks are aphyric.

Acknowledgements

We are grateful to the Captain, crew and scientists on board the CSS John P. Tully for their assistance, and to Chief Scientist Jim Franklin for his support. Sandra Barr and Dick Chase are thanked for providing additional samples. Bob McKay is thanked for assistance with the microprobe analyses. Thorough reviews by W.B. Bryan, L.S. Hollister, and R.F. Martin greatly improved the manuscript. This work was funded by NSERC operating grants to NVW and THP.

References

Allan, J.F., Batiza, R., Perfit, M.R., Fornari, D.J. & Sack, R.O. (1989): Petrology of lavas from the Lamont Seamount Chain and adjacent East Pacific Rise, 10°N. *J. Petrol.* **30**, 1245-1298.

———, Sack, R.O. & Batiza, R. (1988): Cr-rich spinels as petrogenetic indicators: MORB-type lavas from the Lamont seamount chain, eastern Pacific. *Am. Mineral.* **73**, 741-753.

Bender, J.F., Hodges, F.N. & Bence, A.E. (1978): Petrogenesis of basalts from the project FAMOUS area: experimental study from 0–15 kbars. *Earth Planet. Sci. Lett.* **41**, 277-302.

Bryan, W.B. (1979): Regional variation and petrogenesis of basalt glasses from the FAMOUS area, Mid-Atlantic Ridge. *J. Petrol.* **20**, 293-325.

Davis, A.S. & Clague, D.A. (1990): Gabbroic xenoliths from the northern Gorda Ridge: implications for magma chamber processes under slow spreading centres. *J. Geophys. Res.* **95**, 10885-10905.

Davis, E.E., Currie, R. & Sawyer, B. (1987): Bathymetry map 6–1987, northern Juan de Fuca Ridge. *Geol. Surv. Can., Energy, Mines and Resources, Ottawa, Ontario.*

———, Lister, C.R.B. & Lewis, B.T.R. (1976): Seismic structure of the Juan de Fuca Ridge: ocean bottom seismometer results from the median valley. *J. Geophys. Res.* **81**, 3541-3555.

Dixon, J.E. & Clague, D.A. (1986): Gabbroic xenoliths and host ferrobasalt from the southern Juan de Fuca Ridge. *J. Geophys. Res.* **91**, 3795-3820.

Donaldson, C.H. & Brown, R.W. (1977): Refractory megacrysts and magnesian-rich melt inclusions within spinel in oceanic tholeiites: indicators of magma mixing and perental magma composition. *Earth Planet. Sci. Lett.* **37**, 81-89.

Dungan, M.A. & Rhodes, J.M. (1978): Residual glasses and melt inclusions in basalts from DSDP Legs 45 and 46: evidence for magma mixing. *Contrib. Mineral. Petrol.* **67**, 417-431.

Elthon, D. (1984): Plagioclase buoyancy in oceanic basalts: chemical effects. *Geochim. Cosmochim. Acta* **48**, 753-768.

Fisk, M.R., Bence, A.E. & Schilling, J.G. (1982): Major element chemistry of Galapagos Rift Zone magmas and their phenocrysts. *Earth Planet. Sci. Lett.* **61**, 171-189.

Fornari, D.J., Perfit, M.R., Allan, J.F., Batiza, R., Haymon, R., Barone, A., Ryan, W.B.F., Smith, T., Simkin, T. & Luckman, M.A. (1988): Geochemical and structural studies of the Lamont seamounts: seamounts as indicators of mantle processes. *Earth Planet. Sci. Lett.* **89**, 63-83.

Hummler, E. & Whitechurch, H. (1988): Petrology of basalts from the Central Indian Ridge (lat. 25°239S, long. 70°049E): estimates of frequencies and fractional volumes of magma injections in a two-layered reservoir. *Earth Planet. Sci. Lett.* **88**, 169-181.

Kuo, Lung-Chuan & Kirkpatrick, R.J. (1982): Pre-eruption history of phyric basalts from DSDP legs 45 and 46: evidence from morphology and zoning patterns in plagioclase. *Contrib. Mineral. Petrol.* **79**, 13-27.

Leybourne, M.I. & Van Wagoner, N.A. (1991): Heck and Heckle seamounts, northeast Pacific Ocean: high extrusion rates of primitive and highly depleted mid-ocean ridge basalt on off-ridge seamounts. *J. Geophys. Res.* **96**, 16275-16293.

——— & ——— (1992): Volcanism, age and hydrothermal deposits of the West Valley Segment, Juan de Fuca Ridge. *Can. J. Earth Sci.* **29**, 2346-2352.

Nabelek, P.I. & Langmuir, C.H. (1986): The significance of unusual zoning in olivines from FAMOUS area basalt 527–1–1. *Contrib. Mineral. Petrol.* **93**, 1-8.

Pearce, T.H. & Clark, A.H. (1989): Nomarski interference contrast observations of textural details in volcanic rocks. *Geology* **17**, 757-759.

———— & KOLISNIK, A.M. (1990): Observations of plagioclase zoning using interference imaging. *Earth Sci. Rev.* **29,** 9-26.

————, RUSSELL, J.K. & WOLFSON, I. (1987): Laser-interference and Nomarski interference imaging of zoning profiles in plagioclase phenocrysts from the May 18, 1980, eruption of Mount St. Helens, Washington. *Am. Mineral.* **72,** 1131-1143.

RHODES, J.M., DUNGAN, M.A., BLANCHARD, D.P. & LONG, P.E. (1979): Magma mixing at mid-ocean ridges: evidence from basalts drilled near 22°N on the Mid-Atlantic Ridge. *Tectonophys.* **55,** 35-61.

STAKES, D.S., SHERVAIS, J.W. & CLIFFORD, C.A. (1984): The volcanic–tectonic cycle of the FAMOUS and AMAR valleys, Mid-Atlantic Ridge (36°47′N): evidence from basalt glass and phenocryst compositional variations for a steady state magma chamber beneath the valley mid-sections, AMAR 3. *J. Geophys. Res.* **89,** 6995-7028.

STAMATELOPOULOU-SEYMOUR, K., VLASSOPOULOS, D., PEARCE, T.H. & RICE, C. (1990): The record of magma chamber processes in plagioclase phenocrysts at Thera Volcano, Aegean volcanic arc, Greece. *Contrib. Mineral. Petrol.* **104,** 73-84.

TSUCHIYAMA, A. (1985): Dissolution kinetics of plagioclase in the melt of the system diopside – albite – anorthite and the origin of dusty plagioclase in andesites. *Contrib. Mineral. Petrol.* **89,** 1-16.

ULMER, P. (1989): The dependence of the Fe^{2+} – Mg cation-partitioning between olivine and basaltic liquid on pressure, temperature and composition. *Contrib. Mineral. Petrol.* **101,** 261-273.

VAN WAGONER, N.A. & LEYBOURNE, M.I. (1991): Evidence for magma mixing and a heterogeneous mantle on the West Valley Segment of the Juan de Fuca Ridge. *J. Geophys. Res.* **96,** 16295-16318.

VINE, F.J. & WILSON, J.T. (1965): Magnetic anomalies over a young oceanic ridge off Vancouver Island. *Science* **150,** 485-489.

Received March 1, 1993, revised manuscript accepted September 12, 1994.